Noise sources

Edoardo Milotti

December 4, 2023

Here we consider the noise sources that affect the interferometer sensitivity. For this handout, I have taken portions of text from [3, 4, 5].

Noise is extremely relevant in gravitational wave interferometers. To see why, consider a detector like Virgo, with an arm length of 3 km: it responds to a gravitational wave with an amplitude of 10^{-21} with an arm length difference

$$\delta L_{\mathrm{GW}} \sim hL \sim 3 \times 10^{-18}\mathrm{m}. \tag{1}$$

As we have already seen, we can increase the effective path length inside each interferometer arm by using a Fabry-Perot resonator, which increases the effective path length by a factor $\mathcal{F}/\pi$, as long as the period of the gravitational wave is much less than characteristic time of the resonator[1]

$$\tau_p = \frac{L}{c}\frac{\mathcal{F}}{\pi}. \tag{2}$$

In this case, taking the finesse of the Virgo FP cavities, $\mathcal{F} \approx 450$, the photon path is multiplied by about 150, and we find that the arm length difference increases

$$\delta L_{\mathrm{GW}} \sim 4.5 \times 10^{-16}\mathrm{m}, \tag{3}$$

finally, we must be able to control noise at least at this level.

The detector noise level is characterized by the spectral sensitivity, see figure 1 which shows the sensitivity curves of the three interferometers of the LVC network near the end of the O3 observing run (March 2020).

1 Basic description of the main noise sources

This section lists the main categories of noise that affect the interferometers. They do not include more common noise source like electronic noise that must also be kept in check.

---

[1]It can be shown that this holds if the frequency of the gravitational wave $f_{\mathrm{GW}} \ll c/2\pi L$, and that in the opposite case the sensitivity is decreased by a factor $\sqrt{1 + (f_{\mathrm{GW}}/f_{\mathrm{FP}})^2}$, where $f_{\mathrm{FP}} = 1/4\pi\tau_p$, because we average the strain of the gravitational wave over more than one period.
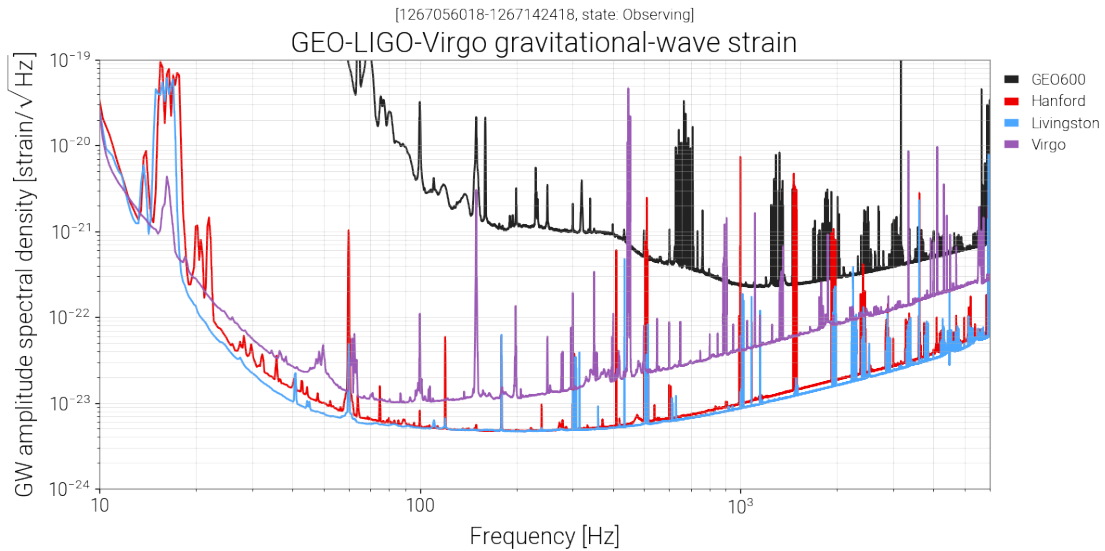
Figure 1: This plot represents the median noise of each interferometer measured over the course of the day, during the final month of the O3 observing run, on March 1st, 2020. The measured output of each interferometer, calibrated to units of gravitational wave strain, is shown as a function of frequency. Since the amplitude of a gravitational wave signal changes with frequency, the shape of this curve determines each detector's sensitivity to incoming gravitational waves. This plot is often referred to as the "noise curve". (Plot from the Gravitational Wave Open Science Center summary status page, https://www.gw-openscience.org/detector_status/day/20200301/)

Ground vibrations. External mechanical vibrations must be screened out. These are a serious problem for interferometers, because interferometers bounce light back and forth between the mirrors, and so each reflection introduces further vibrational noise. **Suspension/isolation systems are based on pendulums. A pendulum is a good mechanical filter for frequencies above its natural frequency.** By hanging the mirrors on pendulums of about 0.5 m length, one achieves filtering above a few Hertz. Since the spectrum of ground noise falls at higher frequencies, this provides suitable isolation. These systems can be very sophisticated. The most ambitious multi-stage isolation system has been developed for the Virgo detector.

Thermal noise. Vibrations of the mirrors and of the suspending pendulum can mask gravitational waves. As with vibrational noise, this is increased by the bouncing of the light between the mirrors. In the gravitational interferometers, the pendulum suspensions have thermal noise at a few Hertz, so measurements are made above 10 Hz. Internal vibrations of the mirrors have natural frequencies of several kHz, which sets an effective upper limit to the observing band. By ensuring that both

kinds of oscillations have very high Q, one can confine most of the vibration energy to a small bandwidth around the resonant frequency, so that at the measurement frequencies the vibration amplitudes are extremely small. This allows interferometers to operate at room temperature. But mechanical Qs of 10^7 or higher are required, and this is technically demanding.

Thermal effects produce other disturbances besides vibration. Some of the mirrors in interferometers are partly transmissive, as is the beam splitter. A small amount of light power is absorbed during transmission, which raises the temperature of the mirror and changes its index of refraction. The resulting "thermal lensing" can ruin the optical properties of the system, and random fluctuations in lensing caused by time-dependent thermal fluctuations (thermo-refractive noise) can appear at measurement frequencies. These effects can limit the amount of laser power that can be used in the detector. Other problems can arise from heating effects in the multiple-layer coatings that are applied to the reflective surfaces of mirrors.

Shot noise. The photons that are used to do interferometry are quantized, and so they arrive at random and make random fluctuations in the light intensity that can look like a gravitational wave signal. At this initial level, we note that

1. The more photons one uses, the smoother the interference signal will be. As a random process, the error improves with the square root of the number N of photons. Using light with a wavelength λ, one can expect to measure to an accuracy of

$$\delta L_{\text{shot}} \sim \lambda/(2\pi\sqrt{N}) \tag{4}$$

   (usually infrared light with $\lambda \sim 1\mu$m is actually used).

2. To measure at a frequency f, one has to make at least $2f$ measurements per second, so one can accumulate photons for a time $1/2f$ (the sampling time). With light power P, one gets

$$N = P/(hc/\lambda)/(2f) \tag{5}$$

   photons.

3. In order that δL_{shot} should be below 10^{-18}m, one needs high laser power. Power-recycling techniques overcome this problem, by using light efficiently. An interferometer actually has two places where light leaves. One is where the interference is measured, the antisymmetric port. The other is the sum of the two return beams on the beam splitter, which goes back towards the input laser (the symmetric port). Normally one makes sure that no light hits the interference sensor, so that only when a gravitational wave passes does a signal register there. This means that all the light normally returns toward the laser input, apart from small losses at the mirrors. By placing a power-recycling mirror in front of the laser, one can reflect this wasted light back in, allowing power to build up in the arms until the laser merely resupplies the

3

mirror losses. This can dramatically reduce the power requirement for the laser. Current interferometers work with laser powers > 30W.

Quantum noise. Shot noise is a quantum noise, and like all quantum noises there is a corresponding conjugate noise. As laser power is increased to reduce shot noise, the position sensing accuracy improves, and one eventually comes up against the Heisenberg uncertainty principle: the fluctuations of the momentum transferred to the mirror by the measurement leads to a disturbance that can mask a gravitational wave (see Fig. 2). **Thus, the uncertainty principle defines the Standard Quantum Limit (SQL) to gravitational wave measurements.** However the SQL can be beaten! To reduce the backaction pressure fluctuation, the quantum state of the light can be modified by "squeezing" the Heisenberg uncertainty ellipse, in order to reduce the effect of this uncertainty on the variable being measured, at the expense of its (unmeasured) conjugate. **The key point here is that we are using a quantum field (light) to measure an effectively classical quantity (gravitational wave amplitude), so we do not need to know everything about our quantum system: we just need to reduce the uncertainty in that part of the quantum field that responds to the gravitational wave at the readout of our interferometer.** Squeezing is currently implemented in both LIGO interferometers and in Virgo.
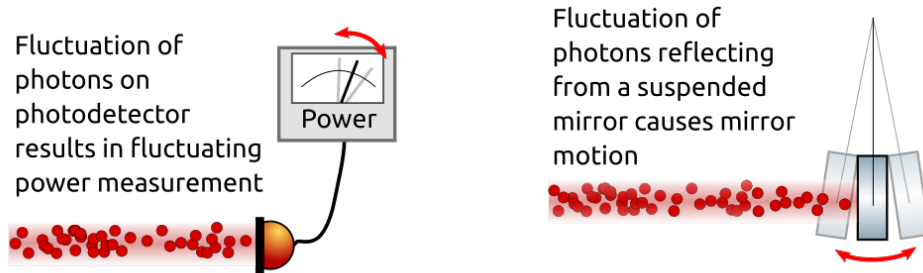

Figure 2: Pictorial representation of shot noise and radiation pressure noise.

The noise listed above are just the most important components of the overall *noise budget* which is schematically illustrated in figure 3
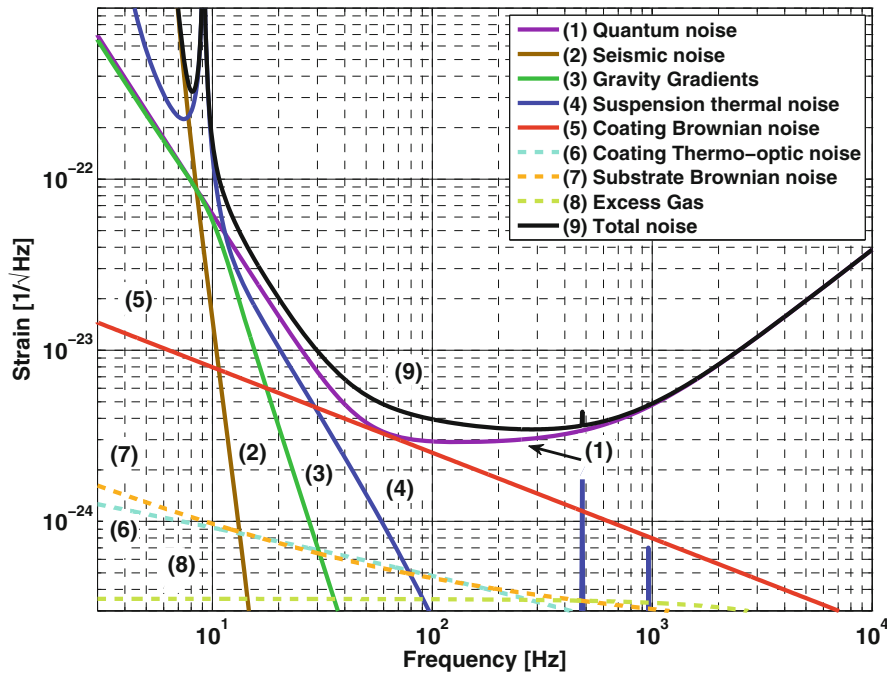
Figure 3: Noise budget of the advanced LIGO broadband configuration as described in R.Abbott et al., AdvLIGO Interferometer Sensing and Control Conceptual Design, Technical note LIGO-T070247-01-I (2008)

2 Noise modeling: thermal noise

The noises described in the previous section can be modeled, and their mechanisms can be manipulated to mitigate them. Here, I illustrate the kind of modeling that can be done in the case of thermal noise, which brings us close to another facet of Einstein's research, that on stochastic processes [1] (see figure 4).

5. *Über die von der molekularkinetischen Theorie*
der Wärme geforderte Bewegung von in ruhenden
Flüssigkeiten suspendierten Teilchen;
von A. Einstein.

———————

In dieser Arbeit soll gezeigt werden, daß nach der molekular-kinetischen Theorie der Wärme in Flüssigkeiten suspendierte Körper von mikroskopisch sichtbarer Größe infolge der Molekularbewegung der Wärme Bewegungen von solcher Größe ausführen müssen, daß diese Bewegungen leicht mit dem Mikroskop nachgewiesen werden können. Es ist möglich, daß die hier zu behandelnden Bewegungen mit der sogenannten „Brownschen Molekularbewegung" identisch sind; die mir erreichbaren Angaben über letztere sind jedoch so ungenau, daß ich mir hierüber kein Urteil bilden konnte.

Figure 4: The starting lines of Einstein's 1905 paper on Brownian motion [1].

Three years after Einstein's paper, Paul Langevin devised a very different description of Brownian motion [2], in the guise of a stochastic differential equation in the time domain, the one-dimensional Langevin equation (see figure 5)

$$m\frac{dv}{dt} = -\gamma v(t) + n(t) \tag{6}$$

where γ is the friction coefficient and n is a zero-mean, Gaussian, white noise process with correlation function $\langle n(t')n(t'')\rangle = \sigma^2\delta(t'-t'')$. This stochastic differential equation can be solved by taking first the ensemble average

$$m\frac{d\langle v\rangle}{dt} = -\gamma\langle v\rangle \tag{7}$$

which can be solved to find the average speed

$$\langle v(t)\rangle_{v_0} = v_0\exp\left(-\frac{\gamma t}{m}\right). \tag{8}$$

Next, we multiply by $x(t)$ and take the ensemble average again

$$\left\langle x\frac{dv}{dt}\right\rangle = -\frac{\gamma}{m}\langle xv\rangle \tag{9}$$

6

Figure 5: The starting lines of Langevin's 1908 paper [2].

and we note that

$$xv = \frac{1}{2}\frac{dx^2}{dt},\tag{10}$$

and

$$x\frac{dv}{dt} = \frac{d}{dt}(xv) - \left(\frac{dx}{dt}\right)^2 = \frac{1}{2}\frac{d^2x^2}{dt^2} - v^2,\tag{11}$$

so that eq. (9) becomes

$$\frac{1}{2}\left\langle\frac{d^2x^2}{dt^2}\right\rangle - \langle v^2\rangle = -\frac{\gamma}{2m}\left\langle\frac{dx^2}{dt}\right\rangle.\tag{12}$$

We simplify the last equation using the equipartition theorem

$$\frac{1}{2}m\langle v^2\rangle = \frac{1}{2}k_B T\tag{13}$$

and we find

$$\left\langle\frac{d^2x^2}{dt^2}\right\rangle + \frac{\gamma}{m}\left\langle\frac{dx^2}{dt}\right\rangle = \frac{2k_B T}{m},\tag{14}$$

which we simplify using an integrating factor

$$\frac{d}{dt}\left(e^{\gamma t/m}\frac{d\langle x^2\rangle}{dt}\right) = e^{\gamma t/m}\frac{2k_B T}{m},\tag{15}$$

7

and finally we integrate with the initial conditions $x(0) = 0$, and $v(0) = v_0$, which imply

$$0 = \langle x\dot{x} \rangle|_{t=0} = \frac{1}{2} \left.\frac{d\langle x^2 \rangle}{dt}\right|_{t=0} = 0$$

so that

$$\frac{d\langle x^2 \rangle}{dt} = \frac{2k_B T}{\gamma} \left(1 - e^{-\gamma t/m}\right) \tag{16}$$

and

$$\langle x^2 \rangle = \frac{2k_B T}{\gamma} \left(t + \frac{m}{\gamma} e^{-\gamma t/m} - \frac{m}{\gamma}\right) \tag{17}$$

which for long times becomes

$$\langle x^2 \rangle \approx \frac{2k_B T}{\gamma} t \tag{18}$$

Now, let's go back to the Langevin equation (6) and integrate it formally using the same integrating factor

$$e^{-\gamma t/m} \frac{d}{dt} \left(e^{\gamma t/m} v(t)\right) = \frac{n(t)}{m} \tag{19}$$

i.e.,

$$v(t) = v(0)e^{-\gamma t/m} + \frac{1}{m} \int_0^t e^{-\gamma(t-t')/m} \, n(t')dt'. \tag{20}$$

Then, squaring and averaging, and finally taking the limit for large t,

$$\langle v^2(t) \rangle = v^2(0)e^{-2\gamma t/m} + \frac{1}{m^2} \int_0^t e^{-\gamma(t-t')/m} e^{-\gamma(t-t'')/m} \langle n(t')n(t'') \rangle dt'dt''$$

$$= v^2(0)e^{-2\gamma t/m} + \frac{\sigma^2}{m^2} \int_0^t e^{-2\gamma(t-t')/m} dt' = v^2(0)e^{-2\gamma t/m} + \frac{\sigma^2}{2\gamma m}(1 - e^{-2\gamma t/m})$$

$$\rightarrow \frac{\sigma^2}{2\gamma m} \tag{21}$$

and using again the equipartition theorem,

$$\langle v^2 \rangle = \frac{k_B T}{m} = \frac{\sigma^2}{2\gamma m} \tag{22}$$

we find

$$\sigma^2 = 2\gamma k_B T. \tag{23}$$

8

From the Wiener-Kintchine theorem, we know that the power spectral density[2] is the Fourier transform of the correlation function, i.e.,

$$S_n(\omega) = \int_{-\infty}^{+\infty} \langle n(t)n(t+\tau)\rangle e^{-i\omega\tau} d\tau = \int_{-\infty}^{+\infty} \sigma^2 \delta(\tau) e^{-i\omega\tau} d\tau = \sigma^2. \tag{25}$$

The last result means that the one-sided spectral density of the noise process is independent of frequency (n is a white noise) and is equal to

$$S_n(\omega) = 4k_B T\gamma. \tag{26}$$

Now consider a thermally excited damped harmonic oscillator described by the equation

$$m\ddot{x} - \gamma\dot{x} + kx = n(t) \tag{27}$$

then the previous results imply that the power spectral density of x is

$$S_x(\omega) = \frac{S_n(\omega)}{(k - m\omega^2)^2 + \gamma^2\omega^2} \tag{28}$$

A sample power spectral density is shown in figure 2 (figure taken from [5]).

The latest result is an example of *fluctuation-dissipation theorem*, so called because it relates fluctuations (described by the power spectral density) with dissipation in the system (expressed by the friction coefficient).

On this basis, many thermal noise sources inside the interferometers have been studied and characterized.

---

[2]Recall that the power spectral density of a signal $s(t)$ is defined by the following formula

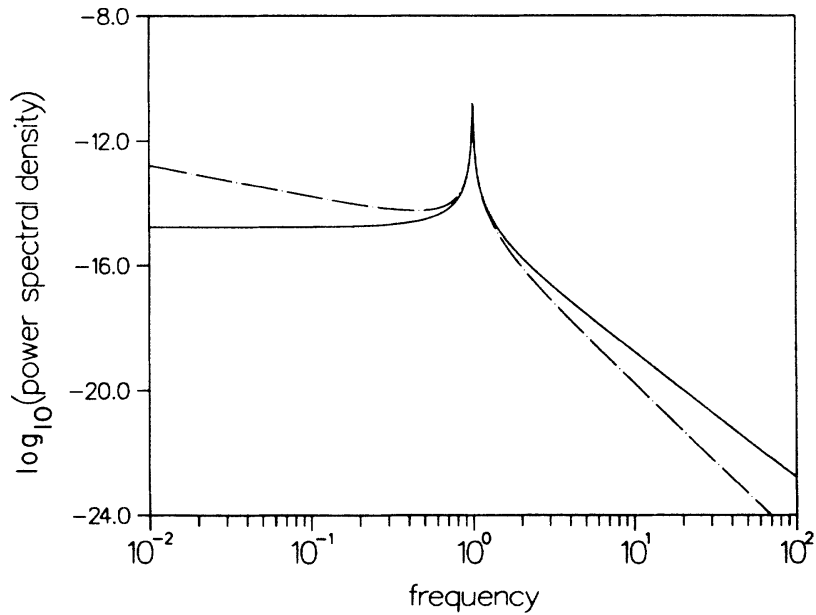$$S(\omega) = \lim_{T\to\infty} \frac{1}{T} \left| \int_{-T/2}^{+T/2} s(t)e^{-i\omega t} dt \right|^2 \tag{24}$$

FIG. 2. Thermal noise power spectra for two mechanical oscillators, each with $m = 1$ g, resonant frequency $\omega_0 = 1$ s^{-1}, and $Q = 100$. The solid line shows the spectrum for an oscillator with damping proportional to velocity. The dash-dotted line shows the spectrum for an oscillator with internal damping characterized by constant $\phi(\omega)$. The units of the power spectral density are cm^2/Hz and of the frequency axis are s^{-1}.

3 Shot noise

Let N_γ be the average number of photons with energy $\hbar\omega_\gamma$ that reach the detector from the laser source during time T. Then, the average power measured during this observation time is

$$P = \frac{1}{T} N_\gamma \hbar\omega_\gamma \qquad (29)$$

It is fair to assume that the actual number of photons is a Poisson variate with variance equal to the average N_γ, so that the standard deviation is $\Delta N_\gamma = \sqrt{N_\gamma}$. The corresponding fluctuation of the measured power is

$$\Delta P_{\text{shot}} = \frac{1}{T} \sqrt{N_\gamma} \hbar\omega_\gamma = \left(\frac{\hbar\omega_\gamma}{T} P \right)^{1/2} \qquad (30)$$

Now, we want to assess the effect of this noise on GW measurements by comparing it with the power received by the photodiode when a GW signal is present.

In our analysis of GW interferometers, we found that a Michelson interferometer with Fabry-Perot arms has signal at the modulation frequency that carries information on GW amplitude

$$P_{\text{out}}(\Omega) = P_{\text{in}} \left[16 J_0(\beta) J_1(\beta) \sin\left(\frac{\Omega}{c} \delta\ell \right) \mathcal{F}_{\text{ac}} \frac{L}{\lambda} \left(1 - \frac{\mathcal{F}_{\text{ac}}}{\pi} \epsilon \right) h \cos(\Omega t + 2\Omega\ell/c) \right], \qquad (31)$$

i.e., a signal with amplitude

$$\Delta P_{\text{out}} = P_{\text{in}} \left| 16 J_0(\beta) J_1(\beta) \sin\left(\frac{\Omega}{c} \delta\ell \right) \mathcal{F}_{\text{ac}} \frac{L}{\lambda} \left(1 - \frac{\mathcal{F}_{\text{ac}}}{\pi} \epsilon \right) h \right|, \qquad (32)$$

and that DC power is also present

$$P_{\text{DC}} \approx P_{\text{in}} J_1^2(\beta). \qquad (33)$$

The DC term is associated with the average shot noise fluctuation

$$\Delta P_{\text{shot}} = \left(\frac{\hbar\omega}{T} P_{\text{in}} \right)^{1/2} |J_1(\beta)| \qquad (34)$$

and therefore the power signal-to-noise ratio (SNR) is

$$\frac{S}{N} = \frac{\Delta P_{\text{out}}}{\Delta P_{\text{shot}}} = \left(\frac{T P_{\text{in}}}{\hbar\omega} \right)^{1/2} \frac{16L}{\lambda} \sin\left(\frac{\Omega}{c} \delta\ell \right) \mathcal{F}_{\text{ac}} \frac{L}{\lambda} \left(1 - \frac{\mathcal{F}_{\text{ac}}}{\pi} \epsilon \right) h \qquad (35)$$

In general, we notice that the higher the power, the larger the SNR: powerful lasers reduce the impact of shot noise!

References

[1] Albert Einstein. Über die von der molekularkinetischen theorie der wärme geforderte bewegung von in ruhenden flüssigkeiten suspendierten teilchen. *Annalen der physik*, 4, 1905.

[2] Paul Langevin. Sur la théorie du mouvement brownien. *Compt. Rendus*, 146:530–533, 1908.

[3] Michele Maggiore. *Gravitational waves: Volume 1: Theory and experiments*. OUP Oxford, 2007.

[4] Bangalore Suryanarayana Sathyaprakash and Bernard F Schutz. Physics, astrophysics and cosmology with gravitational waves. *Living reviews in relativity*, 12:1–141, 2009.

[5] Peter R Saulson. Thermal noise in mechanical experiments. *Physical Review D*, 42(8):2437, 1990.